Ytterbium-Doped Fiber Amplifiers

Rüdiger Paschotta, Johan Nilsson, Anne C. Tropper, and David C. Hanna

***Abstract*—The ytterbium-doped fiber amplifier offers a number of attractive features, including a broad-gain bandwidth and a high efficiency, due in large part to its freedom from various competing processes seen in other rare-earth dopants. Here we discuss the main features that influence design and possible applications of ytterbium-doped fiber amplifiers.**

***Index Terms*— Fiber amplifiers.**

I. Introduction

SINCE ITS invention in 1985, the erbium-doped fiber amplifier [1]–[3] (EDFA) has attracted great interest, principally by virtue of its major commercial applications in the field of communication technology. However, the uses of EDFA's have not been confined to telecommunications and there has been steadily growing interest in, for example, the amplification of pulses to provide a source of very high peak powers. In such a context where the specific wavelength's advantage of the EDFA for telecommunications is no longer relevant, amplifiers based on other rare-earth dopants offer themselves for consideration. Ytterbium-doped fibers are a case in point, and while they have so far been used mainly as lasers [4]–[9], their ability to provide amplification over the very broad wavelength range from ∼975 to ∼1200 nm is expected to generate increasing interest in the near future.

Apart from their broad-gain bandwidth, Yb-doped fiber amplifiers (YDFA's) can offer high output power and excellent power conversion efficiency. Many of the complications which are well-known from erbium-doped amplifiers are avoided: excited state absorption and concentration quenching by interionic energy transfer do not occur, and high doping levels are possible, leading to high gain in a short length of fiber. The broad bandwidth is ideal for the amplification of ultrashort pulses, and the high saturation fluence allows for high pulse energies. There is also a wide range of possible pump wavelengths (∼860 nm ⋯1064 nm), allowing a variety of pumping schemes, including the use of diode lasers or even high-power Nd lasers.

Possible applications of YDFA's include power amplification at special wavelengths (e.g., 1083 nm as required for spectroscopic measurements [10]), small-signal amplifiers in fiber sensing applications, free-space laser communications, and chirped-pulse amplification of ultrashort pulses which can themselves be produced in an Yb-doped fiber laser, as recently demonstrated [11].

Given the growing interest in YDFA's, this paper is aimed at a general discussion of aspects of YDFA's that are of relevance to potential users. While many of the general features of EDFA's, which have been treated very extensively (see, e.g., [2]), are common to YDFA's, nevertheless there are also significant differences that need to be emphasized. The most obvious are of course the differences in spectroscopic features which are reviewed in Section II. While we have aimed to keep the discussion rather general, it is also valuable to have some feel for the magnitude of various relevant quantities for a typical set of fiber parameters and operating conditions; we have specified some of those in Section III. In Section IV, we discuss briefly the question of modeling of YDFA's. The broad range of pump and emission wavelengths offers a considerable diversity of pumping and amplification schemes, and these are discussed in Section V. This is followed by a section on cladding pumping (Section VI), and since there are a number of situations, cladding pumping being one, where conditions point to the use of considerable fiber lengths, Section VII provides a reminder that if stimulated Brillouin scattering is to be avoided in cases with narrow-signal bandwidth, some length constraint also needs to be observed. Section VIII then considers the use of the YDFA in the role of a chirped-pulse amplifier.

II. Spectroscopic Properties

Silica glass, the most common material for the production of fibers, is for most applications an ideal host for Yb^{3+} although other host materials are also the subject of investigation, e.g., fluoride glasses [7] in fiber form and numerous crystalline hosts for use in bulk or waveguide form. We therefore concentrate exclusively on Yb^{3+}:silica fibers in this paper. The spectroscopy of the Yb^{3+} ion is simple compared to other rare-earth ions. For all optical wavelengths, only two level manifolds are relevant: the $^2F_{7/2}$ ground-state manifold and the $^2F_{5/2}$ excited-state manifold. These consist of four and three sublevels, respectively. The corresponding transitions between sublevels are not fully resolved for Yb^{3+} ions in a glass at room temperature because of the strong homogeneous and inhomogeneous broadening. Fig. 1 shows the cross sections for absorption and emission of Yb^{3+} in a germanosilicate glass. The absorption cross sections have been obtained from a white-light absorption spectrum in a fiber; the absolute scaling was calculated from fluorescence saturation data. The spectral shape of the emission was obtained from a

Manuscript received February 6, 1997. The work of J. Nilsson was supported by the Swedish Research Council for Engineering Sciences.

R. Paschotta was with the Optoelectronics Research Centre, University of Southampton, Southampton SO17 1BJ, England, U.K. He is now with the Universität-GH-Paderborn, 33098 Paderborn, Germany.

J. Nilsson was with the Optoelectronics Research Centre, University of Southampton, Southampton SO17 1BJ, England, U.K. He is now with Samsung Electronics, Suwon, South Korea 440–600.

A. C. Tropper and D. C. Hanna are with the Optoelectronics Research Centre, University of Southampton, Southampton SO17 1BJ, England, U.K.

Publisher Item Identifier S 0018-9197(97)04699-X.

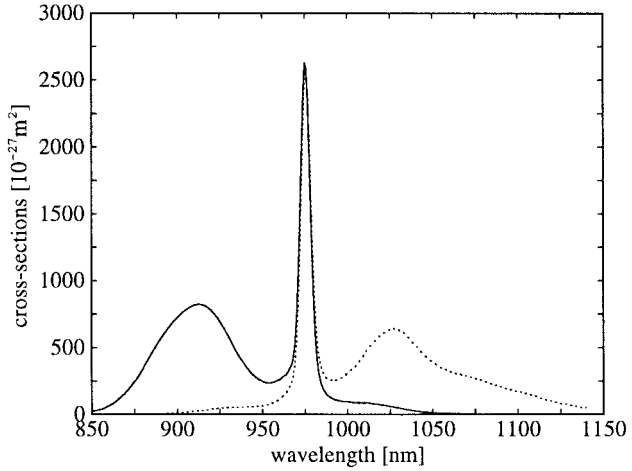

Fig. 1. Absorption (solid) and emission (dotted) cross sections of Yb in germanosilicate glass.

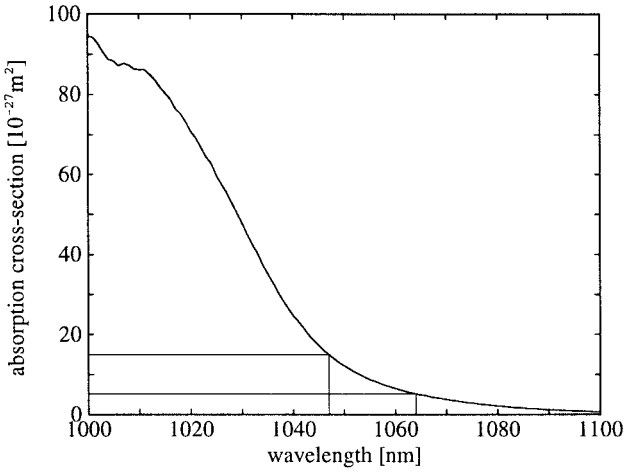

Fig. 2. Absorption cross sections of Yb in germanosilicate glass, with an expanded vertical scale for the long wavelength range. The values at 1064 nm (Nd:YAG) and 1047 nm (Nd:YLF) are indicated.

fluorescence spectrum in the side light of a fiber, thus avoiding any distortion due to reabsorption. The absolute scaling of the emission cross sections was determined by the assumption that absorption and emission cross section are identical at the main peak of 975 nm; this assumption is believed to be correct within a few percent. Because the absorption data are not precise in the weak long-wavelength tail beyond 990 nm, the data in this region is based on values calculated from McCumber theory [12], using the more precise emission data. The higher precision achieved in this way is important for the modeling of amplifiers and lasers pumped at these longer wavelengths, e.g., at 1047 or 1064 nm. Fig. 2 shows the absorption in this range on a magnified scale. The same technique has also been used to calculate precise emission parameters from the absorption data for the region below 960 nm.

It should be noted that the details of absorption and emission spectra depend to some extent on the host glass composition [13], [14]. We have compared the emission spectra of various Yb-doped germanosilicate fibers with differing content of germanium, aluminum, and boron; typical deviations from the cross sections as shown in Fig. 1 are up to about 30%, especially in the range 990–1020 nm. The measured fluorescence decay times of typically around 0.8 ms also vary by about 30% between different fibers; fibers with higher germanium content in the core (introduced to achieve a higher numerical aperture) tend to have shorter lifetimes (and correspondingly larger cross sections) while Yb^{3+} in a pure silicate glass (and also in some phosphosilicate glasses) has a lifetime around 1.5 ms. Moreover, the emission spectra vary to some extent with pump wavelength [8], indicating some inhomogeneous broadening, although the broadening is dominantly homogeneous.

We have reported earlier that in many Yb-doped fibers (from more than one source) a significant fraction of the Yb^{3+} ion population is quenched to a very short lifetime [15]. This effect is not immediately obvious from the fluorescence decay since it is easy to overlook the very weak fluorescence from quenched ions (with continuous excitation) as the fluorescence decay of the other ions is not affected, even when a large fraction of the ion population is quenched. However, the effect manifests itself in a strong nonsaturable loss which has essentially the same spectral shape as the absorption from nonquenched ions. It has been shown that fibers with a low level of quenching can be produced although the physical mechanism responsible for quenching and the procedures needed to minimize it have not yet been identified. YDFA's will be sensitive to the effect especially when they are pumped at the 975-nm absorption peak; significant pump power can be lost via this nonsaturable absorption which does not produce gain. Some detuning of the pump wavelength from the 975-nm peak, effectively reducing the absorption cross section, would then increase the gain efficiency. This follows from the fact that a reduced absorption cross section and hence increased saturation power (for nonquenched ions) would result in reduced saturation, hence an increased fraction of pump power absorbed by nonquenched ions relative to that absorbed by quenched ions. A laser or power amplifier operating on the 975-nm emission would be even more sensitive to the quenching effect.

Another effect which could in principle reduce the gain at higher Yb concentrations is cooperative upconversion [16], a process in which two near Yb^{3+} ions combine their excitation energy to emit a single photon in the green spectral range. However, even in strongly doped fibers (e.g., 10 000 ppm by weight), we have found this process to be too weak to significantly affect the gain.

Excited-state absorption of pump or signal light, or concentration quenching by ion–ion energy transfer processes such as are observed in other rare-earth doped fibers, notably in EDFA's (see, e.g., [17]) does not occur with Yb due to the absence of other energy levels. Only energy migration within the Yb^{3+} population is possible. This could affect the gain efficiency if excitation energy were transported to isolated impurity traps. However, even in fibers with Yb concentrations as high as 20 000 ppm (by weight), energy migration to traps does not appear to be a significant decay route, as otherwise one would not have observed relatively long fluorescence decay times ($\approx$0.8 ms) in fibers where up to 90% of the ions were quenched [15].

III. Some Useful Numbers

In an initial consideration of appropriate design parameters, such as fiber length, dopant concentration, pump power, etc., it is helpful to have some feel for typical magnitudes. So, we present here some parameter values for a typical germanosilicate fiber, i.e., a single-mode fiber with 900-nm cutoff wavelength and a numerical aperture of 0.2, which implies a 3.4-μm core diameter, and an excited-state lifetime of 0.8 ms. For 1000 ppm (by weight) Yb^{3+} concentration in the core, we get the following numbers.

- The unpumped fiber has a small signal absorption of 80.5 dB/m at the 975-nm absorption peak and 26.6 dB/m at the 910-nm absorption peak.
- The pump saturation intensity is that intensity which reduces the pump absorption to half the low-power value and is given by $I_{\mathrm{sat}} = h\nu_p/(\sigma_{12}^{(p)} + \sigma_{21}^{(p)})\tau$. Equivalent to that is the definition as that intensity which produces an upper-level population half that of the high-power ($I \gg I_{\mathrm{sat}}$) value, which is $n_2 = \sigma_{12}^{(p)}/(\sigma_{12}^{(p)} + \sigma_{21}^{(p)})$. Some calculated saturation powers are 0.49 mW for 975 nm, 3.1 mW for 910 nm, and 5.6 mW for 1047 nm.
- Thermalization of the sublevel populations within each manifold is so fast that it can be assumed instantaneous; therefore, we need only specify the fractional populations n_1, n_2 of the lower and upper manifolds, respectively. A strong pump at 910 nm generates 97% upper-state population. Maintaining this population requires an absorbed pump power of 19 mW/m. The gain is then 76 dB/m at 975 nm and 18 dB/m at 1030 nm. (Note that the total gain is limited by amplified spontaneous emission (ASE); see Section V for details.) The stored energy (when released at 975 nm) is 13 μJ/m.
- A strong 975-nm pump creates 50% upper-state population (since absorption and emission cross sections are equal at this wavelength) with a corresponding power dissipation of 9.3 mW/m. This generates a gain of 9 dB/m at 1030 nm, and the stored energy is 7 μJ/m.

IV. Modeling of Yb-Doped Fiber Amplifiers

As long as ASE does not extract significant power and purely homogeneous broadening is assumed, numerical modeling of Yb-doped fiber lasers is very simple. We describe such a numerical model only very briefly because the same models as for Er-doped amplifiers [18]–[20] can be used.

The local Yb upper- and lower-state population are governed by the rate equations

$$\frac{dn_2}{dt} = (R_{12} + W_{12})n_1 - (R_{21} + W_{21} + A_{21})n_2 \quad (1)$$

$$\frac{dn_1}{dt} = -(R_{12} + W_{12})n_1 + (R_{21} + W_{21} + A_{21})n_2 \quad (2)$$

from which we obtain the steady-state values

$$n_2 = \frac{R_{12} + W_{12}}{R_{12} + R_{21} + W_{12} + W_{21} + A_{21}} \quad (3)$$

$$n_1 = 1 - n_2. \quad (4)$$

The transition rates are

$$R_{12} = \sigma_{12}^{(p)} I_p/h\nu_p, \quad R_{21} = \sigma_{21}^{(p)} I_p/h\nu_p \quad (5)$$

$$W_{12} = \sigma_{12}^{(s)} I_s/h\nu_s, \quad W_{21} = \sigma_{21}^{(s)} I_s/h\nu_s \quad (6)$$

where $\sigma_{12}^{(p)}$ and $\sigma_{21}^{(p)}$ are the effective pump absorption and emission cross sections, $\sigma_{12}^{(s)}$ and $\sigma_{21}^{(s)}$ the corresponding values for the signal wavelength, and I_p and I_s are the pump and signal intensities (in $\mathrm{W/m^2}$). For the usual single-mode fibers, reasonable accuracy is achieved with the approximation of constant pump and signal intensities over the cross section of the fiber core if additional overlap factors η_p and η_s are introduced to account for the fact that some fraction of the power propagates in the undoped cladding of the fiber [19], [20].

The gain and loss for pump and signal at a given longitudinal position z along the fiber is then given by the equations

$$\frac{dP_p}{dz} = \eta_p(\sigma_{21}^{(p)} n_2 - \sigma_{12}^{(p)} n_1)N_{\mathrm{tot}} P_p \quad (7)$$

$$\frac{dP_s}{dz} = \eta_s(\sigma_{21}^{(s)} n_2 - \sigma_{12}^{(s)} n_1)N_{\mathrm{tot}} P_s \quad (8)$$

for the pump and signal power, where N_{tot} is the total density (in $\mathrm{m^{-3}}$) of Yb^{3+} ions. We have here assumed the case of an amplifier with copropagating pump and signal. It is then straightforward to propagate the powers from the input end to the output end, using, e.g., the Runge–Kutta formulas. In the case of a counterpropagating signal, the sign of (8) must be reversed, and one can, e.g., propagate the input pump power (at $z = 0$) and an estimate for the output signal power from the pump end to the other end, refining the estimate in an iterative procedure until the given signal input power is reproduced by the calculation at this end [18].

We summarize briefly the technical difficulties encountered when the effect of ASE is included into the model. For each direction of propagation, the growth of ASE must be calculated for several wavelength channels separately because the spectral shape of the ASE can vary strongly due to the wavelength-selective amplification and reabsorption. (The number of ASE channels in the numerical model can be kept relatively small by using the concept of an effective ASE bandwidth [21].) If significant ASE powers are expected, their back-action on the local excited-state population has to be taken into account. An iterative procedure is required to find a self-consistent solution, satisfying all the boundary conditions in the form of given pump and signal input powers and zero ASE power densities starting to grow from each end. ASE powers usually start to have a significant effect on gain when the peak gain reaches about 30–40 dB. For lower gains, a much simpler model which ignores the effect of ASE on the level populations can be used; the propagation equations (7) and (8) can even be solved analytically in this case [20].

V. Amplifier Configurations

The pronounced structure in the Yb absorption and emission spectra has some implications for the design of YDFA's which do not arise in the case of EDFA's: there are distinctly different regimes of operation depending on pump and signal

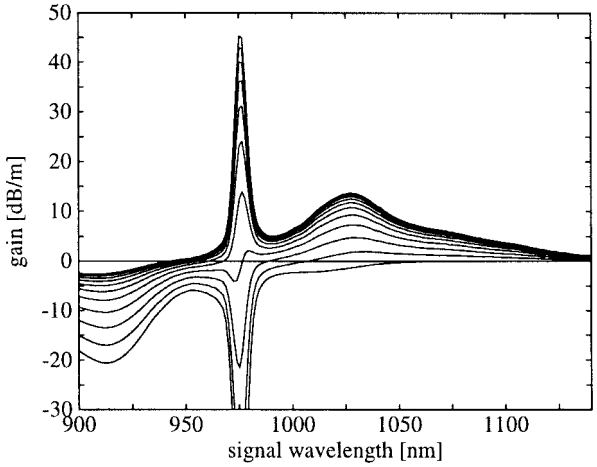

Fig. 3. Calculated gain spectra for a Yb-doped germanosilicate fiber with 900 nm cutoff, NA = 0.2, 1000 ppm Yb (wt.), for different pump powers (in intervals of 3 mW, from 0 to 30 mW) at 910 nm.

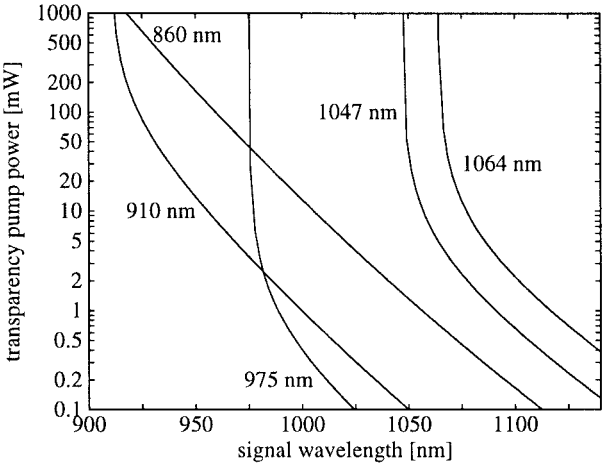

Fig. 4. Transparency pump power versus signal wavelength for various common pump wavelengths, assuming a germanosilicate fiber with 900-nm cutoff and NA = 0.2.

wavelength. The narrow absorption peak at 975 nm, and the broader and weaker peak at 910 nm offer the obvious choices for pump wavelengths. However, longer wavelengths, like 1047 or 1064 nm (where considerable pump power is available in the form of Nd lasers) or even the short wavelengths at ~860 nm or less may be used if availability of suitable diode lasers is a dictating factor. Gain can be achieved on the 975-nm emission peak or over a range of wavelengths on the much broader peak centered at ~1030 nm. Of course, gain is available only at wavelengths longer than the pump wavelength.

Fig. 3 shows the calculated gain in a Yb-doped fiber versus wavelength for different pump powers at 910 nm for which nearly complete inversion can be obtained (a similar diagram was shown in [9]). For short wavelengths around 975 nm, we find a pronounced three-level behavior: without pump power there is strong absorption so that the length of an amplifying fiber for this wavelength would have to be carefully optimized to avoid loss in an unpumped section. On the other hand, for long wavelengths (>1100 nm), one has nearly pure four-level behavior with the gain proportional to the overall upper-state population, and reabsorption in an unpumped fiber is very weak. Optimum efficiency of an amplifier is achieved when the residual pump power at the far end is just sufficient to reach transparency (zero gain) for the signal wave at this point, except if the residual pump light is reflected back at the end in order to achieve higher efficiency. The transparency power versus signal wavelength, given by

$$P_{\text{trans}} = \frac{A_c h\nu_p}{\eta_p(\sigma_{21}^{(s)}\sigma_{12}^{(p)}/\sigma_{12}^{(s)} - \sigma_{21}^{(p)})\tau} \tag{9}$$

(with A_c = core area) is plotted in Fig. 4 for various pump wavelengths and typical fiber parameters (a similar graph is shown in [9]).

In the following discussion of the amplifier, we distinguish between four different cases.

A. 910-nm Pump, Amplification at 975 nm

Very high gain in a short length can be achieved at 975 nm with a pump wavelength around 910 nm. This is a consequence of the large emission cross section at 975 nm, plus the fact that pumping at 910 nm allows essentially all of the Yb population to be excited to the upper manifold. The total gain will be limited only by ASE to roughly 45 dB. The transparency power is only ≈3.5 mW (see Fig. 4), and ≈4.6 mW of absorbed pump power will already generate 10-dB gain. The rather narrow 3-dB amplification bandwidth, only about 2.25 nm for 40 dB or 2.6 nm for 30-dB peak gain, limits the potential use of this amplifying transition.

B. 910-nm Pump, Amplification at ~1000 ··· 1150 nm

A much broader amplification bandwidth is available in the long-wavelength region peaked at ~1030 nm which includes several wavelengths of interest, such as 1047 and 1053 nm (Nd:YLF), 1064 nm (Nd:YAG), or 1083 nm (for spectroscopy on metastable helium). A strong 910-nm pump leads to 97% upper-state population, i.e., nearly the maximum possible gain per unit length. However, the gain at 975 nm is then very strong (see Fig. 5), with the consequence that ASE around 975 nm limits the gain available at longer wavelengths. One way to get around this limitation is to pump at 975 nm; this is discussed in Section V-C, and Fig. 6 shows the gain at 1030 nm versus pump power for both pump wavelengths (as well as the gain at 975 nm for 910-nm pump). Another way is to use a double-pass configuration, with the signal but not the ASE (at 975 nm) reflected back after the first pass, so that ideally the signal can have twice the gain of a single-pass configuration.

There is another possibility, potentially providing higher gain: the 975-nm ASE can be suppressed by a medium providing loss at this wavelength. Er-doped silica fibers happen to have an absorption peak which matches this wavelength quite well; at the same time, the erbium would not generate loss at either 910 nm or the signal wavelength. Therefore, the 975-nm ASE problem could be solved by splicing several pieces of Yb-doped fiber and Er-doped fiber together. The

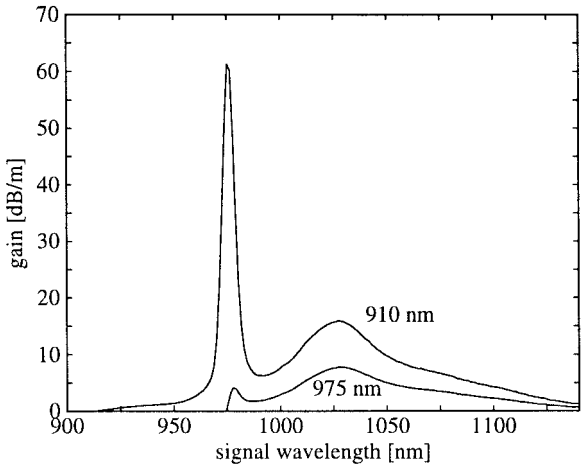

Fig. 5. Calculated gain spectra for a Yb-doped germanosilicate fiber with 900-nm cutoff, NA = 0.2, 1000 ppm Yb (wt.), for 910-nm and 975-nm pumps with a power high enough to saturate the whole length of fiber.

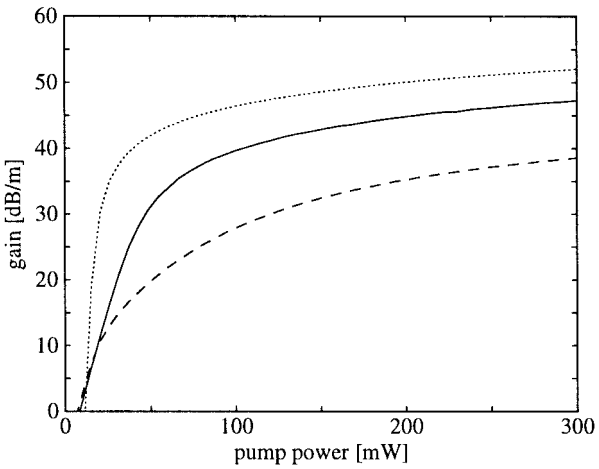

Fig. 6. Small-signal gain versus pump power of an YDFA, calculated from a model which takes ASE into account, for fiber parameters as in Section III. Solid curve: gain at 1030 nm for 975-nm pump, 6-m length. Dashed curve: gain at 1030 nm for 910-nm pump, 6-m length (showing strong saturation by 975-nm ASE). Dotted curve: gain at 975 nm for 910-nm pump, 1-m length.

splice losses would not lead to a significant reduction of gain, provided that fibers with suitable parameters (in particular with similar numerical aperture) are used.

In principle, the generation of significant ASE power does not necessarily affect the performance if it is reabsorbed and thus contributes to the signal gain in sections with lower population inversion. For forward ASE (propagating in the direction of the pump), this can be achieved simply by using a sufficiently long fiber while backward ASE could be prevented from extracting significant power at the pump end by the use of a fiber grating at this point which would reflect back ASE around 975 nm. Our simulations have shown that significant improvements could be achieved even with a grating reflection bandwidth of 1 nm, but a detailed discussion of this method would go beyond the scope of this paper.

C. 975-nm Pump, Amplification at ∼1000 ··· 1150 nm

The most direct way to avoid the problem with 975-nm ASE is to use a 975-nm pump. As absorption and emission cross section are essentially equal at this wavelength, a maximum of 50% upper state population is achieved for strong pumping, i.e., for powers well above the saturation power which in fact has the rather low value of ∼0.5 mW (calculated for fiber parameters of 900-nm cutoff and NA = 0.2). Therefore, the maximum gain per unit length at 1030 nm or longer wavelengths is about half the gain obtained with 910-nm pumping (see Fig. 5). It is now limited only by ASE around 1030 nm, i.e., the gain at 1030 nm is limited to roughly 45 dB (see Fig. 6). This is still a serious limitation of the gain achievable at longer wavelengths; for example, the gain at 1083 nm (interesting for spectroscopy of metastable helium) is then only ∼14 dB. Higher gains at long wavelengths could only be achieved with some scheme of ASE filtering, either in a double-pass configuration or with some absorber, as discussed in Section V-B. The principle of reflecting backward ASE at the pump end with a fiber grating (as discussed in Section V-B) seems not very practical in this case, basically because it would take a long fiber length to reabsorb the forward ASE.

The pump absorption is very efficient if a 975-nm pump is used. This is due to the very high absorption cross section. The upper state population is held nearly constant at 50% from the pump end up to the point where the saturation power (∼0.5 mW) is reached. At this point, the upper-state population is 25%, and the residual pump power is very quickly absorbed in the following fiber section. The negative side of the strong absorption cross section is, however, the sensitivity to the quenching effect mentioned in Section II.

If the pump power is chosen so high that the entire fiber is saturated (i.e., significant pump is left unabsorbed), the gain saturation is very weak, i.e., the gain stays high even for relatively large signal output powers. The gain saturation is then significantly weaker than for EDFA's (because of the higher pump cross sections relative to the emission cross sections) and also weaker than for a 910-nm pump. This is illustrated in Fig. 7 where the gain versus signal input power is compared between amplifiers with a 975-nm pump and a 910-nm pump (with half the length in the second case in order to obtain similar unsaturated gain).

D. 1047-nm or 1064-nm Pump, Amplification Around ∼1100 nm

Despite the very small absorption in this wavelength region, a 1047-nm pump (Nd:YLF) or even a 1064-nm pump (Nd:YAG) can be used to generate gain at longer wavelengths. For accurate predictions, it is necessary to use absorption cross-section values calculated from the emission data using the McCumber theory (see Section II). As the absorption cross section is much smaller than the emission cross section for these wavelengths, the saturated upper-state population is very low, only 3.4% for 1047-nm pumping or 1.7% for 1064-nm pumping at high pump powers. The saturation power is in this case determined mainly by the pump emission cross section and is therefore not very high; for typical fiber parameters (see Section III), it is calculated as 4.3 mW at 1047 nm and 6.0 mW at 1064 nm. The achieved gain per unit length is

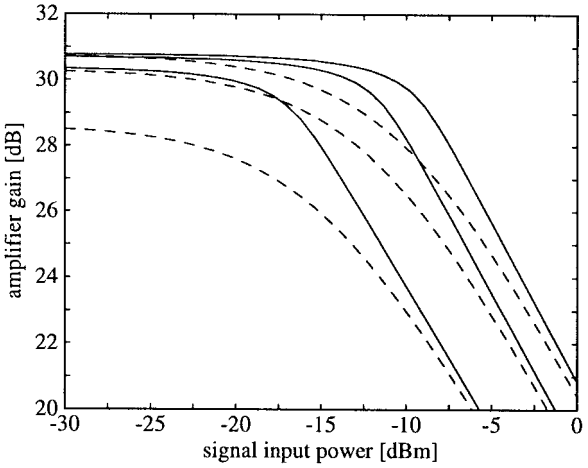

Fig. 7. Gain at 1030 nm versus signal input power, calculated for fiber with 900-nm cutoff, NA = 0.2, 2000 ppm (wt.) Yb. Solid curves: 2-m-long amplifier with a 975-nm pump; 50-, 100-, and 150-mW pump power. Dashed curves: 1-m-long amplifier with a 910-nm pump, same pump powers. It is assumed that the 975-nm ASE is suppressed.

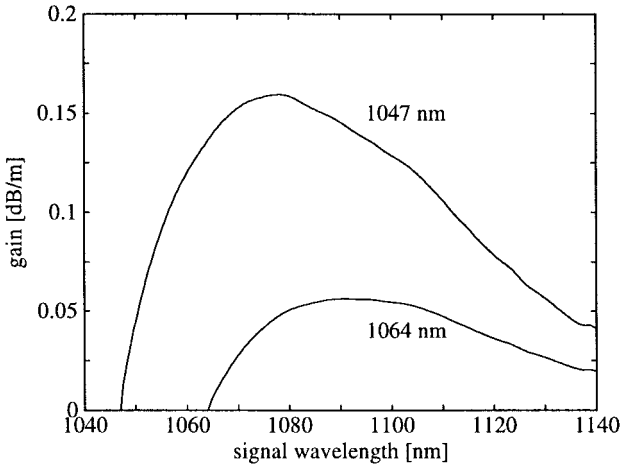

Fig. 8. Calculated gain spectra for a Yb-doped germanosilicate fiber with 900-nm cutoff, NA = 0.2, 1000 ppm Yb (wt.), for 1047- and 1064-nm pumps with high (saturating) power.

rather small but (for sufficiently high dopant concentration) still larger than a typical fiber loss of $\sim 0.01 \cdots 0.05$ dB/m, so that by using a long length one can obtain both significant gain and good gain efficiency. Indeed, we have made a $\sim$50-m-long fiber laser with 2400 ppm (wt.) Yb^{3+}, pumped at 1047 nm with a high reflector for the signal wavelength at the pump input end, which reaches threshold with $\sim$7-dB single-pass gain at 1100 nm for about 60 mW of launched pump. Fig. 8 shows calculated gain spectra for pumping at 1047 or 1064 nm, assuming perfectly homogeneous broadening. Some deviations from these spectra are expected in practice.

Note that the use of a long pump wavelength for amplification around 1100 nm has the advantage of not producing high gain and consequently ASE at shorter wavelengths as would happen, e.g., with a 975-nm pump.

VI. Cladding-Pumped Fiber Amplifiers

For fiber amplifiers capable of high-output-power operation (more than $\sim$1 W), so-called double-clad fibers [22] can be used. Such fibers usually have a single-mode core in which the signal wave propagates, surrounded by a larger multimode undoped inner cladding into which the pump light is launched. The modes of the inner cladding have some overlap with the doped core so that the pump light can be absorbed there. The main advantages of this scheme are that higher powers can be coupled into a multimode core (because of the larger spot size), the pump source (e.g., a high-power diode laser) does not need to emit a single spatial mode; the pump launch efficiency can be very high and the alignment tolerances relatively uncritical.

A cladding-pumped Yb-doped laser has already been demonstrated [23]. An output power of 500 mW at 1040 nm has been achieved with the very high conversion efficiency of 80% with respect to incident power. The round-trip gain of 14 dB, needed to reach laser threshold, required 75 mW of incident pump power. A cladding-pumped amplifier with Er:Yb codoped fiber has been used to amplify a train of femtosecond pulses to 260-mW average power [24]. There are prospects for several watts of output power to be obtained from such devices.

In general, three-level transitions, causing significant reabsorption of signal in weakly pumped regions, are less favorable for cladding-pumped operation. This is because the pump intensity at the end of the amplifier must be still high enough to avoid signal reabsorption, which in the case of a double-clad fiber (with its large pumped area) results in a high residual pump power and consequently low efficiency (back reflection of residual pump power is often not feasible). However, at least for longer signal wavelengths ($>$1040 nm) the ytterbium transition has a predominantly four-level nature, and efficient cladding-pumped operation is possible. For shorter signal wavelengths it is possible to increase the power efficiency by using a double-pass configuration where both pump and signal wave are reflected back at the end of the amplifier.

Because of the lower pump absorption per unit length, cladding-pumped devices tend to require a longer fiber length. Provided the fiber loss can be kept small (less than 0.01 dB/m are achievable), this need not create a problem. In some cases, as discussed in Section VII, the extra length can give problems via stimulated Brillouin scattering.

VII. Stimulated Brillouin Scattering

The signal wave traveling in a fiber amplifier generates Brillouin gain for a backward traveling Stokes wave with slightly lower optical frequency [25] (by $\approx$18 GHz for a 1-μm signal). Because of the small bandwidth of the Brillouin gain ($\sim$38 MHz in silica fibers for a 1-μm signal), only signals with high spectral density can lead to high Brillouin gain and generation of a Brillouin wave which can extract significant power. This is the case especially when a single-frequency signal is amplified to a high power level. For example, there is interest in amplifying a single-frequency beam at 1083 nm (as used for spectroscopy on metastable helium) to high powers [10], and the consideration of Brillouin gain is important in such a case.

For propagation in undoped optical fiber, the Brillouin wave has to build up from quantum fluctuations and can extract significant power only when the Brillouin gain reaches about 70–80 dB [25]. In an amplifying fiber, however, the Brillouin Stokes wave also experiences laser gain, and in addition the spontaneous emission of the amplifier provides a seed for the Brillouin wave. In this situation, a Brillouin gain as low as 40 dB may be enough to extract significant power and limit the amplifier gain. The effect of stimulated Brillouin scattering has been investigated numerically for distributed Er-doped amplifiers [26]; a similar analysis could be applied to the Yb-doped amplifier.

Using the numbers given in [25], together with typical parameters of Yb-doped amplifying fibers (in particular, a 3.4-μm core diameter, see Section III), we find that the Brillouin gain is $\sim$18 dB/m per watt of signal power (at 1040 nm), provided that the signal bandwidth is less than the Brillouin bandwidth of 38 MHz. This number emphasizes the need to restrict the length of a high-power fiber amplifier if it is to be used for amplification of a single-frequency signal. As amplifiers intended for output powers of several watts will usually use cladding-pumped schemes (see Section VI) which tend to require longer fiber lengths, relatively high Yb concentrations will be needed to keep the fiber short and thus the Brillouin gain low enough. It may be necessary to increase the bandwidth of the signal wave, e.g., by introducing a strong phase modulation (effectively distributing the signal power over several frequency components) which can be removed with a second modulator after the amplifier.

VIII. Chirped-Pulse Amplification

In recent years, the chirped-pulse amplification scheme [27] has made possible the generation of extremely high pulse powers [28]. A single ultrashort pulse ($\sim$10$\cdots$500-fs duration) from a mode-locked source is stretched in time by using a dispersive element which introduces a strong chirp. This chirped pulse can then be amplified to a high energy without reaching too high a peak power which could cause unwanted nonlinear effects or even damage the amplifier medium. After the last amplifier stage, the pulse is recompressed with a dispersive grating pair so that the resulting pulse now has both high energy and short duration. Peak powers of several terawatts have been demonstrated and are now used for a variety of applications involving, e.g., the generation of strong ultrashort coherent pulses in the VUV or X-ray wavelength region [28]. Such sources have so far been realized with Ar-ion pumped Ti:sapphire lasers and amplifiers [29], Nd:glass [30], Cr:LiSAF [31], and KrF [32]. For some applications, somewhat lower pulse energies in the order of 1 mJ should be sufficient, so one can envisage a more compact and completely diode-pumped system based on a Yb-doped oscillator, a Yb-doped fiber amplifier stage, followed by a Yb:silica planar waveguide amplifier. Indeed recent demonstrations have been made, both of a YDFA for high pulse energy [33] and a Yb-doped mode-locked fiber oscillator [11] producing femtosecond pulses. For this scheme, the oscillator would generate pulses with an energy of $\sim$1 nJ at 1030 nm, and the fiber amplifier (after single pulse selection and then pulse stretching) would provide a gain of $\sim$40 dB, resulting in $\approx$10-μJ pulses. For such high pulse energies, the signal mode area must be kept large enough to operate the amplifier below the saturation fluence of

$$F_{\mathrm{sat}} = \frac{h\nu_s}{\sigma_{21}^{(s)} + \sigma_{12}^{(s)}} \sim 0.3\,\mu\mathrm{J}/\mu\mathrm{m}^2, \quad \text{at 1030 nm} \qquad (10)$$

as otherwise the pulse shape could be deformed. The damage fluence may be of the same order (30 J/cm^2) but has not been reached so far. With a low NA of 0.08, the signal mode area is $\approx 6{\cdot}10^{-11}$ m^2 and the saturation energy is then 18 μJ so that 10 μJ pulses from a fiber amplifier stage are possible. Indeed, [33] reports 12-μJ pulses from an Yb-doped amplifier (although recompression was not demonstrated).

The energy which can be stored in a fiber amplifier is normally limited by ASE and can be roughly estimated as the maximum gain ($\sim$40 dB) divided by the gain efficiency which is typically 1.5 dB/μJ for a YDFA operating at 1030 nm. This results in $\sim$26 μJ of extracted energy, i.e., not much more than obtained already. This value is better than for neodymium but significantly lower than for erbium. However, we have recently demonstrated a new fiber design which reduces the gain efficiency (by placing the dopant in a ring around the fiber core) and thus increases the energy storage capability [34]. In the first experiments with such a fiber, we could demonstrate the ability to extract over 60 μJ of pulse energy, and significantly higher pulse energies are expected to be possible in the near future. Therefore, the stored energy of a YDFA is not necessarily limited by ASE to values below those for an EDFA if such a design is used.

We estimate that further amplification of the pulses to $\sim$1 mJ is possible in a planar Yb:glass waveguide amplifier which could, because of the long excited-state lifetime, be pumped with a 20-W diode bar in continuous or quasi-continuous operation. The peak power would then be in the order of 10 GW. Although these peak powers are significantly lower than those available from large flash-lamp and Ar-ion pumped bulk systems, they should still be interesting for a variety of applications which would profit from the compactness, low cost, and reliability of a fully diode-pumped system. For higher powers, it is also possible to operate a Yb-based oscillator/amplifier system at 1053 nm so that flash-lamp-pumped Nd:glass power amplifier stages could be used to generate more energetic pulses.

Chirped-pulse amplification in fibers has already been demonstrated in the case of Er-doped fibers [35], even in cladding-pumped Yb:Er-doped fibers [24], but so far not with Yb-doped fibers in the 1-μm region. The possibility of amplifying further the output of a Yb-doped system in a Yb-doped planar waveguide promises significantly higher peak powers for this approach.

IX. Conclusion

YDFA's offer prospects for a number of interesting applications in the near future, based on the broad amplification bandwidth and efficient performance, free from a number of competing processes encountered with other rare-earth

dopants. As these advantages of Yb become more widely appreciated, it is likely to find wider use. Here we have aimed our discussion at a survey of the potential applications of YDFA's, as well as at outlining some design considerations.

ACKNOWLEDGMENT

The authors thank D. J. Richardson for useful discussions.

REFERENCES

[1] R. J. Mears, L. Reekie, I. M. Jauncey, and D. N. Payne, "Low-noise erbium-doped fiber amplifier operating at 1.54 μm," *Electron. Lett.*, vol. 23, pp. 1026–1028, 1987.
[2] E. Desurvire, *Erbium-Doped Fiber Amplifiers*. New York: Wiley, 1994.
[3] M. J. F. Digonnet, Ed., *Rare Earth Doped Fiber Lasers and Amplifiers*. New York: Marcel Dekker, 1993.
[4] D. C. Hanna, R. M. Percival, I. R. Perry, R. G. Smart, P. J. Suni, J. E. Townsend, and A. C. Tropper, "Continuous-wave oscillation of a monomode ytterbium-doped fiber laser," *Electron. Lett.*, vol. 24, pp. 1111–1113, 1988.
[5] D. C. Hanna, R. M. Percival, I. R. Perry, R. G. Smart, P. J. Suni, and A. C. Tropper, "An ytterbium-doped monomode fiber laser: broadband tunable operation from 1.010 μm to 1.162 μm and three-level operation at 974 nm," *J. Mod. Opt.*, vol. 37, pp. 517–525, 1990.
[6] J. C. Mackechnie, W. L. Barnes, D. C. Hanna, and J. E. Townsend, "High power ytterbium (Yb^{3+})-doped fiber laser operating in the 1.12 μm region," *Electron. Lett.*, vol. 29, pp. 52–53, 1993.
[7] J. Y. Allain, M. Monerie, H. Poignant, and T. Georges, "High-efficiency ytterbium-doped fluoride fiber laser," *J. Non-Crystalline Solids*, vol. 161, pp. 270–273, 1993.
[8] S. Magne, M. Druetta, J. P. Goure, J. C. Thevenin, P. Ferdinand, and G. Monnom, "An ytterbium-doped monomode fiber laser: amplified spontaneous emission, modeling of the gain and tunability in an external cavity," *J. Lumin.*, vol. 60, pp. 647–650, 1994.
[9] H. M. Pask, R. J. Carman, D. C. Hanna, A. C. Tropper, C. J. Mackechnie, P. R. Barber, and J. M. Dawes, "Ytterbium-doped silica fiber lasers: versatile sources for the 1–1.2 μm region," *IEEE J. Select. Topics Quantum Electron.*, vol. 1, pp. 2–13, 1995.
[10] R. Paschotta, D. C. Hanna, P. DeNatale, G. Modugno, M. Inguscio, and P. Laporta, "Power amplifier for 1083 nm using ytterbium doped fiber," *Opt. Commun.*, vol. 136, pp. 243–246, 1997.
[11] V. Cautaerts, D. J. Richardson, R. Paschotta, and D. C. Hanna, "Stretched pulse Yb^{3+}: silica fiber laser," *Opt. Lett.*, to be published.
[12] D. E. McCumber, "Einstein relations connecting broadband emission and absorption spectra," *Phys. Rev. A*, vol. 136, pp. 954–957, 1964.
[13] H. Takebe, T. Murata, and K. Morinaga, "Compositional dependence of absorption and fluorescence of Yb^{3+} in oxide glasses," *J. Amer. Ceram. Soc.*, vol. 79, pp. 681–687, 1996.
[14] M. J. Weber, J. E. Lynch, D. H. Blackburn, and D. J. Cronin, "Dependence of the stimulated emission cross section of Yb^{3+} on host glass composition," *IEEE J. Quantum Electron.*, vol. QE-19, pp. 1600–1607, 1983.
[15] R. Paschotta, J. Nilsson, P. R. Barber, J. E. Caplen, A. C. Tropper, and D. C. Hanna, "Lifetime quenching in Yb doped fibers," *Opt. Commun.*, vol. 136, pp. 375–378, 1997.
[16] S. Magne, Y. Ouerdane, M. Druetta, J. P. Goure, P. Ferdinand, and G. Monnom, "Cooperative luminescence in an ytterbium-doped silica fiber," *Opt. Commun.*, vol. 111, pp. 310–316, 1994.
[17] J. Nilsson, P. Blixt, B. Jaskorzynska, and J. Babonas, "Evaluation of parasitic upconversion mechanisms in Er^{3+}-doped silica-glass fibers by analysis of fluorescence at 980 nm," *J. Lightwave Technol.*, vol. 13, pp. 341–349, 1995.
[18] B. Pedersen, A. Bjarklev, J. H. Povlsen, K. Dybdal, and C. C. Larsen, "The design of erbium-doped fiber amplifiers," *J. Lightwave Technol.*, vol. 9, pp. 1105–1112, 1991.
[19] C. R. Giles and E. Desurvire, "Modeling erbium-doped fiber amplifiers," *J. Lightwave Technol.*, vol. 9, pp. 271–283, 1991.
[20] C. Barnard, P. Myslinski, J. Chrostowski, and M. Kavehrad, "Analytical model for rare-earth-doped fiber amplifiers and lasers," *IEEE J. Quantum Electron.*, vol. 30, pp. 1817–1830, 1994.
[21] E. Jaunart and P. Crahay, "Accurate EDFA modeling using a simple method," *Opt. Quantum Electron.*, vol. 27, pp. 881–886, 1995.
[22] E. Snitzer, H. Po, F. Hakimi, R. Tumminelli, and B. C. McCollum, "Double-clad offset core Nd fiber laser," in *Optical Fiber Sensors, 1988 OSA Tech. Dig. Ser.* Washington, DC: Opt. Soc. Amer., 1988, vol. 2, paper PD5.
[23] H. M. Pask, J. L. Archambault, D. C. Hanna, L. Reekie, P. St. J. Russell, J. E. Townsend, and A. C. Tropper, "Operation of cladding-pumped Yb^{3+}-doped silica fiber lasers in 1 μm region," *Electron. Lett.*, vol. 30, pp. 863–865, 1994.
[24] J. D. Minelly, A. Galvanauskas, M. E. Fermann, D. Harter, J. E. Caplen, Z. J. Chen, and D. N. Payne, "Femtosecond pulse amplification in cladding-pumped fibers," *Opt. Lett.*, vol. 20, pp. 1797–1799, 1995.
[25] D. Cotter, "Stimulated Brillouin scattering in monomode optical fiber," *Opt. Commun.*, vol. 4, pp. 10–19, 1983.
[26] M. F. Ferreira, "Effect of stimulated Brillouin scattering on distributed fiber amplifiers," *Electron. Lett.*, vol. 30, pp. 40–42, 1994.
[27] D. Strickland and G. Mourou, "Compression of amplified chirped optical pulses," *Opt. Commun.*, vol. 56, pp. 219–221, 1985.
[28] M. D. Perry and G. Mourou, "Terawatt to petawatt subpicosecond lasers," *Science*, vol. 264, pp. 917–924, 1994.
[29] K. Yamakawa, P. H. Chiu, A. Magana, and J. D. Kmetec, "Generation of high peak and average power femtosecond pulses at a 10 Hz repetition rate in a titanium-doped sapphire laser," *IEEE J. Quantum Electron.*, vol. 30, pp. 2698–2705, 1994.
[30] K. Yamakawa, H. Sugio, H. Daido, M. Nakatsuka, Y. Kato, and S. Nakai, "1 Hz, 1 ps, terawatt Nd:glass laser," *Opt. Commun.*, vol. 112, pp. 37–42, 1994.
[31] P. Beaud, M. Richardson, E. J. Miesak, and B. H. T. Chai, "8-TW 90-fs Cr:LiSAF laser," *Opt. Lett.*, vol. 18, pp. 1550–1552, 1993.
[32] I. N. Ross, A. R. Damerell, E. J. Divall, J. Evans, G. J. Hirst, C. J. Hooker, J. R. Houliston, M. H. Key, J. M. D. Lister, K. Osvay, "A 1 TW KrF laser using chirped pulse amplification," *Opt. Commun.*, vol. 109, pp. 288–295, 1994.
[33] D. T. Walton, J. Nees, and G. Mourou, "Broad-bandwidth pulse amplification to the 10-μJ level in an ytterbium-doped germanosilicate fiber," *Opt. Lett.*, vol. 21, pp. 1061–1063, 1996.
[34] J. Nilsson, R. Paschotta, J. E. Caplen, and D. C. Hanna, "Yb^{3+}-ring-doped fiber for high-energy pulse amplification," *Opt. Lett.*, to be published.
[35] M. E. Fermann, A. Galvanauskas, and D. Harter, "All-fiber source of 100-nJ subpicosecond pulses," *Appl. Phys. Lett.*, vol. 64, pp. 1315–1317, 1994.

Rüdiger Paschotta was born in Tailfingen, Germany, in 1965. He received the diploma degree in physics and the Ph.D. degree for his work in the fields of nonlinear optics and quantum optics from Konstanz University in 1991 and 1994, respectively.

From 1994 to 1996, he was working at the Optoelectronics Research Centre, University of Southampton, England, on fiber lasers and amplifiers. He is now with the Universität-GH-Paderborn, Paderborn, Germany.

Johan Nilsson received the M. Sc. degree in engineering physics from Chalmers University of Technology, Gothenburg, Sweden, in 1989 and the Ph.D. degree in optics from the Royal Institute of Technology, Stockholm, Sweden, in 1994 for work on optical amplification.

From 1994 to 1995, he developed erbium-doped fiber amplifiers at the Samsung Advanced Institute of Technology in Suwon, Korea. He is has worked on fiber and waveguide lasers and amplifiers at the Optoelectronics Research Centre, University of Southampton, England, until early 1997, and he is now with Samsung Electronics, Suwon, South Korea.

Anne C. Tropper, for photograph and biography, see p. 126 of the February 1997 issue of this JOURNAL.

David C. Hanna, photograph and biography not available at the time of publication.